SPECTROPHOTOMETRIC STUDY OF COMPLEX EQUILIBRIA AND DETERMINATION OF LEAD(II) WITH 4-(2-PYRIDYLAZO)RESORCINOL

Zdenka KLEČKOVÁ, Marie LANGOVÁ and Josef HAVEL

Department of Analytical Chemistry,
Purkyně University, 611 37 Brno

Received October 24th, 1977

Dedicated to Profesor A. Okáč, corresponding member of the Czechoslovak Academy of Sciences on the occasion of his 75th birthday.

The complex equilibria of 4-(2-pyridylazo)resorcinol with Pb^{2+} ions in aqueous solutions were studied spectrophotometrically. The composition, molar absorption coefficients and equilibrium constants of the $PbLH^{+}$ and PbL chelates were found from absorbance curves by graphical methods and by numerical computation. The conditions for the spectrophotometric determination of Pb^{2+} with this reagent were checked.

One of the first heterocyclic azodyes, 4-(2-pyridylazo)resorcinol (PAR) is used and valued for its high sensitivity in reactions with a number of metal ions, in spite of its difficult preparation and complicated purification. The reaction with Pb^{2+} ions is also of analytical importance and is used both for the spectrophotometric determination of Pb^{2+} in aqueous solutions[1,2], where PbI_2 can be separated by extraction into methyl isobutyl ketone and back-extracted into water prior to the determination[3], and also for visual[4] and spectrophotometric[5] indication of the end-point in EDTA titration of Pb^{2+}. Complexes with composition M : L = 1 : 1 and 1 : 2 were found spectrophotometrically and potentiometrically in solutions of Pb^{2+} with PAR (ref.[4,6]).

This work is concerned with the spectrophotometric study of the reaction of Pb^{2+} ions with PAR in aqueous solutions in order to complete earlier findings on complex equilibria, especially in solutions with excess ligand, and to check on conditions and parameters for the spectrophotometric determination of Pb^{2+} with this reagent. The complex equilibria were evaluated using the KANKARE program[14,15] newly modified for the Tesla 200 computer and other methods.

EXPERIMENTAL

Chemicals and Instruments

The stock solution of *p.a.* lead(II) nitrate was standardized by EDTA titration using xylenol orange, 4-(2-pyridylazo)resorcinol (Lachema, Brno) was purified by double recrystallization from methyl alcohol. Its purity was checked by thin-layer chromatography on Silufol R plates

impregnated with EDTA in benzene–acetone (9 : 2) and benzene–methanol (9 : 1) systems and by spectrophotometric titration with a copper(II) nitrate solution at pH 3·5 (0·5M formate buffer) and 520 mm. The purified substance contained 91·5% monosodium PAR salt. The stock solution prepared by dissolving a weighed amount in water was used for one week. The ionic strength of I 0·1 was adjusted with potassium nitrate. The pH was adjusted with nitric acid or potassium hydroxide.

Spectrophotometric measurements were carried out on SFD-2 (USSR) or Unicam SP 700 (England) instruments with 10 mm glass cells; the pH was measured on a PHM 4d Radiometer instrument with a G 202B glass electrode and a K401 saturated calomel electrode protected against penetration of Pb^{2+} ions by a 1M-KNO_3 liquid salt bridge.

Study of Complex Equilibria

Graphical Analysis

The absorbance-pH curves and concentration dependences $A = f(c_L)$ were evaluated by direct and logarithmic analysis using the transformations[7] for experimental conditions where one complex equilibrium predominates. For the equilibrium

$$m\,M + n\,LH_x \rightleftharpoons M_mL_nH_z + q\,H^+ \qquad (A)$$

with equilibrium constant

$$k_{nm} = [M_mL_nH_z][H^+]^q/[M]^m[LH_x]^n \qquad (1)$$

and in solutions with excess metal ions ($c_M \gg c_L$) for mononuclear complexes ($m = 1$), the following equations were used

$$A = \varepsilon_n c_L/n - Z^n(A - A_{0L})(A_{0L}/c_L - 1)^{n-1}[H]^q/(nA - \varepsilon_n c_L)^{n-1} k_n\varepsilon_n c_M\,. \qquad (2)$$

$$\log[Z^n(A - A_{0L})(\varepsilon_n - nA_{0L}/c_L)^{n-1}/(\varepsilon_n c_L - nA)^n] = q\,pH + \log k_n + \log c_M\,. \qquad (3)$$

In solutions with excess ligand ($c_L \gg c_M$), the transformations (*4*) and (*5*) were used:

$$c_M/(A - A_{0L}) = 1/\varepsilon_n + [H]^q\,Z/k_n\varepsilon_n c_L^n\,, \qquad (4)$$

$$\log[(A - A_{0L})\,Z/(\varepsilon_n c_M - A - A_{0L})] = q\,pH + \log k_n + n\log c_L\,. \qquad (5)$$

For solutions with a small reagent excess,

$$(A - A_{0L})/c_M = (\varepsilon_n - nA_{0L}/c_L) - \\ - (A - A_{0L})[H]^q\,Z^n(1 - nA_{0L}/\varepsilon_n c_L)^n/(c_L - nA/\varepsilon_n)^n\,k_n c_M \qquad (6)$$

$$\log [(A - A_{0L}) Z^n / c_M(\varepsilon_n - nA_{0L}/c_L) - (A - A_{0L})] (c_L - nA/\varepsilon_n)^n = \\ = q\ \mathrm{pH} + \log k_n - n \log (1 - nA_{0L}/\varepsilon_n c_L) . \qquad (7)$$

For the complex transition

$$M_m L_n H_z \rightleftharpoons M_m L_n H_{z-q} + q H^+ \qquad (B)$$

with constant

$$k_{ak} = [M_m L_n H_{z-q}][H]^q / [M_m L_n H_z] \qquad (8)$$

and for solutions with excess of metal ions ($c_M \gg c_L$) and $m = 1$, the transformations

$$c_L/A = n/\varepsilon_2 + (nA - \varepsilon_1 c_L)[H]^q / A\varepsilon_2 k_{ak} , \qquad (9)$$

$$\log (1/\varepsilon_2 c_L - A) = q\ \mathrm{pH} + \log k_{ak} - \log (\varepsilon_2 - \varepsilon_1) \qquad (10)$$

are valid, while for solutions with $c_L \gg c_M$, equations (*11*) and (*12*):

$$c_M/(A - A_{0L}) = 1/\varepsilon_1 + [\varepsilon_2 c_M - (A - A_{0L})]\, k_{ak}/(A - A_{0L})[H]^q , \qquad (11)$$

$$\log \{[(A - A_{01}) - \varepsilon_1 c_M]/[\varepsilon_2 c_M - (A - A_{0L})]\} = q\ \mathrm{pH} + \log k_{ak} . \qquad (12)$$

For equimolar solutions equations (*13*)–(*15*) were applied:

$$c_L/A = n/\varepsilon_2 + (nA - \varepsilon_1 c_L)[H]^q / A k_n \varepsilon_2 , \qquad (13)$$

$$c_L/A = n/\varepsilon_1 - (\varepsilon_2 c_L - nA)\, k/A[H]^q \varepsilon_1 , \qquad (14)$$

$$\log [(nA - \varepsilon_1 c_L)/(\varepsilon_2 c_L - nA)] = \log \varkappa + q\ \mathrm{pH} . \qquad (15)$$

Graphical analysis of the absorbance-pH curves of the reagent was carried out according to the equations

$$c_L/A = 1/\varepsilon_{LH3} + (A - \varepsilon_{LH2} c_L) K_{a1}/A[H]\, \varepsilon_{LH3} , \qquad (16)$$

$$c_L/A = 1/\varepsilon_{LH2} + (A - \varepsilon_{LH3} c_L)[H]/A K_{a1} \varepsilon_{LH2} , \qquad (17)$$

$$\log (A - \varepsilon_{LH2} c_L)/(\varepsilon_{LH3} c_L - A) = \mathrm{pH} + \log K_{a1} . \qquad (18)$$

Symbols: $Z = 1 + [H]/K_{a1}$, in equations (*2*)–(*5*); $Z = 1 + K_{a2}/[H] + [H]/K_{a1}$ in equations (*6*) and (*7*); ε_{LH2} and ε_{LH3} are the molar absorption coefficients of the LH_2 and LH_3^+ reagent forms, respectively, $K_{a1} = [LH_2][H]/[LH_3^+]$; $K_{a2} =$

$= [LH][H]/[LH_2]$; ε_1, ε_2, ε_n are the molar absorption coefficients of the MLH and ML or $M(LH_2)$, and ML_2 chelates, A_{0L} the absorbance of the reagent alone under the same conditions.

Numerical Computer Analysis of Absorbance Curves

The constant values and molar absorption coefficients were calculated from continuous variation plots by the JOB program[8], based on the linear regression of the straight line equation for the transformed Job curves for formation of 1 : 1 complexes and by the JOBCON program[9,10]; using general regression method for the determination of the most probable complex composition and stability constant. The absorbance curves were evaluated by the PRCEK T200 program[11,12] which applies the same transformations (*1*)–(*18*) as the above mentioned graphical methods and constructs the straight lines applying the linear least squares method. The RANKANAL[13] and KANKARE[14] programs based on matrix analysis were employed for analyzing larger sets of absorbance data (at a greater number of wavelengths) in dependence on the pH, reagent or metal concentration, and for sets of spectra. The RANKANAL program yields the order of the absorbance matrix and thus the number of absorbing species in solution.

In addition the KANKARE program, yields the values of the equilibrium constants for coloured complexes present in the solution, as well as the values of their molar absorption coefficients, from non-linear regression of the concentration data matrix. A version of the KANKARE program modified for the TESLA 200 computer[8,15] was employed in this work. Distribution diagrams, *i.e.* the composition of the solutions for particular concentrations of the components found from known equilibrium constant values, were computed using the HALTAFALL program[16] in the broader HALTAFALL-SPEFO version[17–19].

The STAT program[20] was used for evaluating linear calibration curves by the least squares method. All the computations were carried out on a TESLA 200 computer laboratory of the Technical University in Brno.

Acid–Base Equilibria of 4-(2-*Pyridylazo*)*resorcinol*

The dissociation constants of individual forms of the reagent in water were found from absorbance-pH curves of a $2{\cdot}85 \cdot 10^{-5}$M solution of PAR at an ionic strength of *I* 0·1 and at 25°C by graphical analysis and computation using the PRCEK T200 and KANKARE programs (Table I).

Complex Equilibria of Pb^{2+} and 4-(2-Pyridylazo)resorcinol

Absorption Spectra

The absorption curves of a $6{\cdot}50 \cdot 10^{-5}$M PAR solution with increasing Pb^{2+} concentration in the range $0-6{\cdot}50 \cdot 10^{-3}$M at pH 4·35 with an isosbestic point at 450 nm indicate the transition of the reagent (primarily in the LH_2 form) into a complex with λ_{max} 515 and 410 nm (Fig. 1). These curves were evaluated by the KANKARE program for 20 wavelengths over the range 380–540 nm. The data agreed with the assumed equilibria:

$$LH_2 + H^+ = LH_3^+ ; \quad LH_2 - H^+ = LH^- ;$$

$$LH_2 + Pb^{2+} - H^+ = PbLH^+ .$$

The absorption curve computed by the KANKARE program for quantitative formation of the $PbLH^+$ complex under the given conditions (Fig. 1, curve *12*) agrees well with the experimental curve (Fig. 1, curve *11*). The equilibrium constant value is given in Table II.

A further series of absorption curves for $c_L = 3{\cdot}16 \cdot 10^{-5}$M and c_M increasing in the range $0-3{\cdot}16 \cdot 10^{-5}$M at pH 10·3 with an isosbestic point at 455 nm characterize

Table I

Acid–Base and Spectral Characteristics of PAR in Water at I 0·1 and 25°C

Ligand form	Dissociated group	pK_a	λ_{max}	ε/mmol^{-1} cm^2 (515 nm)
LH_3^+	>NH$^+$ (pyridinium cation)	3·03 ± 0·05[a]; 3·02 ± 0·03[b]; 3·15[b]; 2·66[f]; 3·1[g]; 3·02[h]	394	3 782
LH_2		5·57 ± 0·05[a]; 5·44 ± 0·01[c]; 5·46[c]; 5·48[f]; 5·6[g]; 5·56[h]	387	2 852
LH^-	*o*-OH	11·95 ± 0·04[a]; 12·02 ± 0·03[d]; 11·97[e] 12·31[f]; 11·9[g]; 11·98[h]	413	547
L^{2-}		—	488	24 480

[a] From the KANKARE program at 410, 430, 460, 490, 515, 525, 540 nm; [b] found by graphical analysis and by the T200 PRCEK program at 430, 460 and 490 nm; [c] found by graphical analysis and by the T200 PRCEK T200 program at 410 and 430 nm; [d] by the PRCEK T200 program at 460, 490, 515 and 525; [e] by graphical analysis at 490 and 525 nm; [f] see ref.[6,21]; [g] see ref.[5]; [h] see ref.[22].

the transition of the reagent (LH^- with λ_{max} 410 nm) into a complex (λ_{max} 518 nm) with a higher molar absorption coefficient than for the equilibria at pH 4·35 (Fig. 2). In treatment of this data by the KANKARE program, the minimization process did not converge either for formation of the PbL chelate or for other models considering both PbL and simple or mixed hydroxo complexes of Pb^{2+}. The computation failed either because of other competing equilibria (complex, or possibly hydrolytic) or because of unsuitable choice of the initial estimates of the equilibrium parameters used in the computation.

*Graphical and Numerical Analysis of the Absorbance-*pH *Curves*

The two ascending branches of the absorbance-pH curves of solutions of Pb^{2+} and PAR containing an excess of one of the components indicate gradual formation and transition of at least two complex species (Fig. 3).

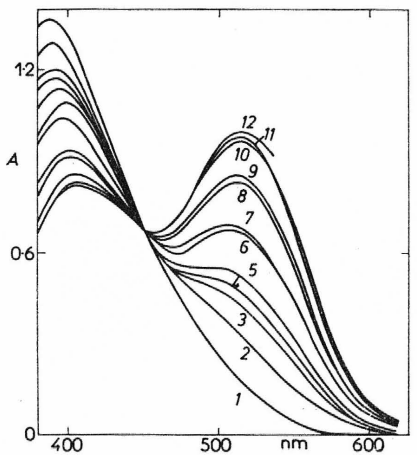

FIG. 1

Absorption Curves for a PAR Solution with Increasing Pb^{2+} Concentration at pH 4·35 $c_L = 6{\cdot}50 \cdot 10^{-5}$M- c_M: curve *1* 0, *2* $3{\cdot}25 \cdot 10^{-5}$M, *3* $4{\cdot}23 \cdot 10^{-5}$M, *4* $5{\cdot}20 \cdot 10^{-5}$M, *5* $5{\cdot}86 \cdot 10^{-5}$M, *6* $6{\cdot}50 \cdot 10^{-5}$M, *7* $1{\cdot}30 \cdot 10^{-4}$M, *8* $3{\cdot}25 \cdot 10^{-4}$M, *9* $5{\cdot}20 \cdot 10^{-4}$M, *10* $1{\cdot}30 \cdot 10^{-3}$M, *11* $6{\cdot}50 \cdot 10^{-3}$M, *12* curve calculated by the KANKARE program for quantitative formation of the $PbLH^+$ complex.

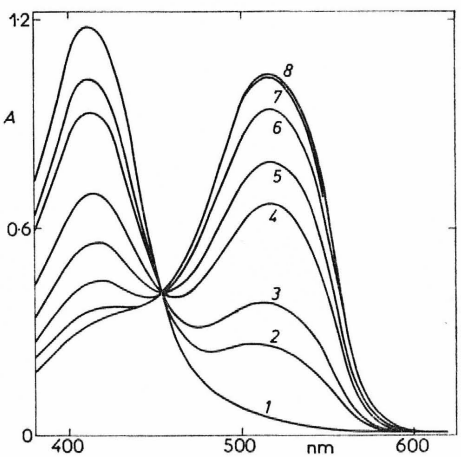

FIG. 2

Absorption Curves for PAR Solution with Increasing Pb^{2+} Concentration at pH 10·30 $c_L = 3{\cdot}16 \cdot 10^{-5}$M, c_M: curve *1* 0, *2* $6{\cdot}23 \cdot 10^{-6}$M, *3* $9{\cdot}46 \cdot 10^{-6}$M, *4* $1{\cdot}58 \cdot 10^{-5}$M, *5* $2{\cdot}21 \cdot 10^{-5}$M, *6* $2{\cdot}53 \cdot 10^{-5}$M, *7* $2{\cdot}85 \cdot 10^{-5}$M, *8* $3{\cdot}16 \cdot 10^{-5}$M.

Analysis of the pH *Curves in the Region* pH 1–4

Graphical analysis of the pH curve for $c_L = 6{\cdot}51 \cdot 10^{-5}$M and $p_M = c_M/c_L = 99{\cdot}9$ in the range pH 2·2 = 2·9 and of the curve with $c_L = 2{\cdot}44 \cdot 10^{-5}$M and $p_M = 10{\cdot}1$ in the range pH = 3·0–4·2 at 515 nm employing equations (*2*) and (*3*) and analysis of the pH curve of solutions with $c_M = 1{\cdot}90 \cdot 10^{-5}$M, $p_L = c_L/c_M = 16{\cdot}1$ in the range pH 3·0–4·3 at 540 nm using equations (*4*) and (*5*) yielded linear transformation dependences, unit slopes of the logarithmic analysis and coinciding values of the molar absorption coefficients and equilibrium constants that verify the equilibrium

$$Pb^{2+} + LH_2 \rightleftharpoons PbLH^+ + H^+ . \qquad (C)$$

Computation of the pH curves for solution with $c_L = 6{\cdot}51 \cdot 10^{-5}$M and $p_M = 99{\cdot}9$ in the range pH 1·6–3·2 at 515, 525 and 540 nm and for solution with $c_M = 1{\cdot}90 \cdot 10^{-5}$M and $p_L = 16{\cdot}1$ at 540 and 560 nm using the PRCEK T200 program as well as evaluation of the curves with $p_M = 99{\cdot}9$ in the interval pH 0·9–3·3 employing the KANKARE program for 16 wavelengths in the range 400–600 nm also confirmed equilibrium (*C*). The values of the equilibrium constant and molar absorption coefficients of the $PbLH^+$ chelate are given in Tables II and III.

Analysis of the pH *Curves in the Interval* pH 5–7

Graphical analysis of the absorbance pH curve of solutions with $c_M = 1{\cdot}90 \cdot 10^{-5}$M and $p_L = 16{\cdot}1$ (Fig. 4) in the range pH 5·9–7·0 at 532 and 540 nm employing equations (*4*) and (*5*) as well as evaluation by the PRCEK T200 program yielded a linear dependence for $q = 1$ and the slope of the logarithmic plot $q = 1{\cdot}05$, con-

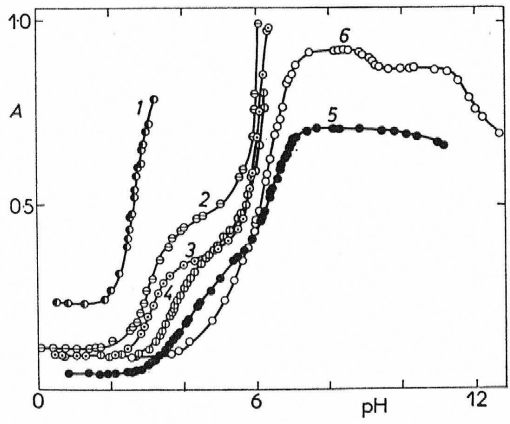

FIG. 3

Absorbance-pH Curves of Pb^{2+} Solutions Containing PAR 515 nm

Curve *1* $c_L = 6{\cdot}51 \cdot 10^{-5}$M, p_M 99·9; *2* $c_L = 2{\cdot}85 \cdot 10^{-5}$M, p_M 98·3; *3* $c_L = 1{\cdot}98 \cdot 10^{-5}$M, $p_M \doteq 100$; *4* $c_L = 2{\cdot}44 \cdot 10^{-5}$M, $p_M \doteq 10{\cdot}1$; *5* $c_M = 1{\cdot}90 \cdot 10^{-5}$M, $p_L \doteq 16{\cdot}1$; *6* $c_M = c_L = 2{\cdot}44 \cdot 10^{-5}$M.

TABLE II

Equilibrium and Stability Constants for the $PbLH^+$ Complex

K	log K
$k_{11H} = [MLH][H]/[M][LH_2]$	$-0{\cdot}19^a$; $-0{\cdot}08^b$; $-0{\cdot}11^c$; $-0{\cdot}16^d$; $-0{\cdot}20^e$; $-0{\cdot}10^f$; $-0{\cdot}10^g$; $-0{\cdot}07^h$; $-0{\cdot}09^i$; $-0{\cdot}14^j$; $-0{\cdot}41^k$; $-0{\cdot}34^l$; $-0{\cdot}29^m$; $-0{\cdot}31^n$
Average:	$-0{\cdot}12$ (*from values* a – j)
$K_{1H} = [MLH]/[M][LH]$	$11{\cdot}83^p$
$K^*_{1H} = [MLH]/[M][LH^*]$	$5{\cdot}45^q$; $5{\cdot}16^k$; $5{\cdot}23^l$

[a,b,c] $A = f(\text{pH})$, $c_L = 6{\cdot}51 \cdot 10^{-5}$M, $p_M = 99{\cdot}9$; [a] KANKARE, pH 1·5–3·3; $\lambda = 400$–600 nm (16 values); [b] PRCEK T200, pH 2·2–3·3, $\lambda \neq 515, 525, 540$ nm; [c] graphical analysis, pH 2·2 to 2·9, $\lambda = 515$ nm; [d,e] $A = f(\text{pH})$, $c_L = 2{\cdot}44 \cdot 10^{-5}$M, $p_M = 10{\cdot}1$; [d] KANKARE, pH 0·7–6·1, $\lambda = 460$–540 nm (14 values); [e] graphical analysis, pH 3·0–4·3, $\lambda = 515$ nm; [f,g,h] $A = f(\text{pH})$, $c_M = 1{\cdot}90 \cdot 10^{-5}$M, $p_L = 16{\cdot}1$; [f] KANKARE, pH = 1·1–7·8, $\lambda = 515$–570 nm (10 values); [g] PRCEK T200, pH 3·0–4·3, $\lambda = 540$–560 nm; [h] graphical analysis, pH 3·0–4·3, $\lambda = 540$ nm; [i] $A = f(c_L)$, $c_M = 6{\cdot}67 \cdot 10^{-5}$M, $c_L = 6{\cdot}52 \cdot 10^{-5}$M–$3{\cdot}26 \cdot 10^{-4}$M, pH 4·25, graphical analysis, $\lambda = 540$ nm; [j] $A = f(\lambda)$, $c_L = 6{\cdot}50 \cdot 10^{-5}$M, $c_M = 0$–$6{\cdot}50 \cdot 10^{-3}$M, KANKARE, $\lambda = 380$ to 540 nm, (20 values); [k,l,m,n] Job curves, $c_L + c_M = 9{\cdot}34 \cdot 10^{-5}$M, $\lambda = 515$ nm; [k] JOB T200, pH = 4·90; [m] KONVAR, pH = 4·90; [l] JOB T200, pH = 5·30; [n] KONVAR, pH = 5·30; [p] from the equation $K_{1H} = k_{11}/K_{a3}$ (LH, reagent anion formed by dissociation of the *o*-hydroxyl group); [q] from the equation $K_{1H} = k_{11}/K_{a2}$ (LH* anion formed by dissociation of the *p*-hydroxyl group).

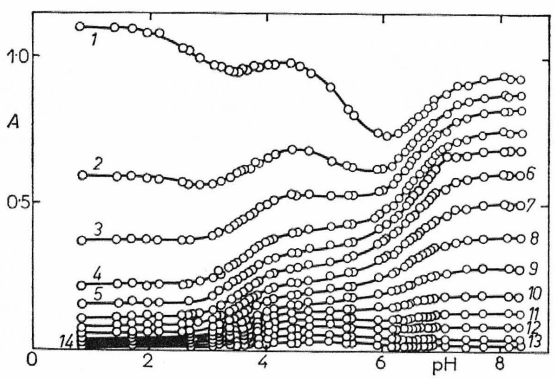

FIG. 4

Absorbance-pH Curve of Pb^{2+} Solutions Containing PAR

$c_M = 1{\cdot}90 \cdot 10^{-5}$M, p_L 16·1; Curve *1* 515 nm, *2* 525 nm, *3* 532 nm, *4* 540 nm, *5* 545 nm, *6* 550 nm, *7* 555 nm, *8* 560 nm, *9* 565 nm, *10* 570 nm, *11* 575 nm, *12* 580 nm, *13* 590 nm, *14* 600 nm.

TABLE III

Molar Absorption Coefficients for the $PbLH^+$ Chelate

Conditions	$\varepsilon \cdot 10^{-4}$, $mmol^{-1}\ cm^2$		
	515 nm	525 nm	540 nm
$A = f(\lambda)$, pH 4·35 $c_L = 6{\cdot}50 \cdot 10^{-5}$M $c_M = 0-1{\cdot}30 \cdot 10^{-3}$M	1·56[a]	1·56[a]	1·46[a]
$A = f(\mathrm{pH})$ $c_L = 6{\cdot}51 \cdot 10^{-5}$M $p_M = 99{\cdot}9$	1·21[a] 1·40[b] 1·29[c]	1·16[a] 1·35[a]	0·99[a] 1·11[b]
$A = f(\mathrm{pH})$ $c_M = 1{\cdot}90 \cdot 10^{-5}$M $p_L = 16{\cdot}1$	1·68[a]	1·41[a]	1·13[a] 1·30[b] 1·33[c]
Average:	*1·43*	*1·37*	*1·22*

[a] KANKARE program; [b] PRCEK T200; [c] graphical analysis.

TABLE IV

Equilibrium and Stability Constant Values for the PbL Complex

K	$\log K$
$k_{12} = [ML][H]^2/[M][LH_2]$ *Average*:	−6·48[a]; −6·44[b]; −6·56[c]; −6·59[d]; *−6·52*
$K_{ak} = [ML][H]/[MLH]$ *Average*:	−6·54[e]; −6·43[f]; −6·40[g]; −6·40[h]; −6·40[i] *−6·43*
$K_1 = [ML]/[M][L]$	10·96[k]

[a,g] $A = f(\mathrm{pH})$, KANKARE, 1st branch $c_L = 6{\cdot}51 \cdot 10^{-5}$M, $p_M = 99{\cdot}9$, 2nd branch $c_L = 2{\cdot}04 \cdot 10^{-5}$M, $p_M = 97{\cdot}3$, pH 0·8–6·2, $\lambda = 480-570$ nm (11 values); [b,h,i] $A = f(\mathrm{pH})$, $c_M = 1{\cdot}90 \cdot 10^{-5}$M, $p_L = 16{\cdot}1$, [b] KANKARE, pH 1·5–7·8, $\lambda = 515-570$ nm (10 values); [h] graphical analysis, pH 6·20–6·95, $\lambda = 540$ nm; [i] PRCEK T200, pH 6·2–6·9, $\lambda = 532$ and 540 nm; [c,d] Job Curves, $c_M + c_L = 9{\cdot}34 \cdot 10^{-5}$M, pH = 11·85, $\lambda = 515$ nm; [c] KONVAR; [d] JOB T200; [e,f] $A = f(\mathrm{pH})$, $c_L = 1{\cdot}98 \cdot 10^{-5}$M, $p_M = 100$, pH = 5·65–6·65, $\lambda = 515$ nm; [e] PRCEK T200, [f] graphical analysis, [g] $A = f(\mathrm{pH})$, $c_L = 2{\cdot}04 \cdot 10^{-5}$M, $p_M = 97{\cdot}3$, pH 5·6–6·6, graphical analysis, $\lambda = 515$ nm; [k] from the equation $K_1 = k_{12}K_{a2} \cdot K_{a3}$.

firming formation of the PbL chelate according to equilibrium (*D*)

$$PbLH^+ \rightleftharpoons PbL + H^+ . \qquad (D)$$

Similarly, evaluation of this pH curve using the KANKARE program for 14 wavelengths in the interval 515–570 nm confirmed the presence of the PbL complex, while models including chelates $Pb(LH)_2$, PbL_2 or PbL(LH) in addition to $PbLH^+$ and PbL were found unsuitable in the computation. These 1 : 2 complexes were eliminated because the sum of the squares of the deviations of the calculated and measured curves for these models is higher than that for 1 : 1 complexes and also because the standard deviations of the equilibrium constant values for $Pb(LH)_2$, PbL_2 and PbL(LH) complexes are much higher than the actual values.

The equilibrium constant values for the PbL chelate are given in Table IV. The molar absorption coefficient values calculated from the second ascending branch of the pH curve for $p_L = 16{\cdot}1$ are 10–20% higher than the values obtained from the horizontal branch of the same and other dependences (Table V) probably because of the effect of interfering equilibria which are more marked in solutions with excess Pb^{2+}.

In computation treatment of the absorbance pH curves of solutions with excess Pb^{2+} ions (pH curve with $c_L = 2{\cdot}04 \cdot 10^{-5}$M, $p_M = 97{\cdot}3$, pH 5·5–6·5, the curve with $c_L = 1{\cdot}98 \cdot 10^{-5}$M, $p_M = 100$, pH 5·6–6·7 and the curve with $c_L = 2{\cdot}44 \cdot 10^{-5}$M, $p_M = 10{\cdot}1$, pH 4·6–6·2) for assumed equilibrium (*D*) using the PRCEK T200 program at 515, 525 and 540 nm and the KANKARE program at 14 wavelengths in the interval 400–600 nm, the molar absorption coefficient values were found to be 40–120% higher than the average value from other dependences and the values of the standard deviations of the equilibrium constants were several orders larger than the constants. Graphical analysis employing equation (*9*) yielded improbably high values of the molar absorption coefficient for the PbL chelate (up to $8{\cdot}3 \cdot 10^4$ at 515 nm). Using the KANKARE program, models including hydrolytic species $PbOH^+$, $Pb(OH_2)$, Pb_2OH^{3+} and $Pb_4(OH)_4^{4+}$ (ref.[26]) in addition to the $PbLH^+$ and PbL complexes were evaluated; however, the minimization process did not converge.

The anomalies in solutions with excess Pb^{2+} in neutral medium may be caused by poor measuring reproducibility and it is also possible that mixed hydroxo complexes of Pb^{2+} with PAR are formed.

Because of the overlapping of the equilibria, it was even not possible to evaluate the individual complexes using the ascending branch of the pH curve for equimolar solutions of Pb^{2+} and PAR ($c_L = c_M = 2{\cdot}44 \cdot 10^{-5}$M).

Absorbance–Ligand-Concentration Plots

The concentration plot for $c_M = 6{\cdot}75 \cdot 10^{-5}$M and c_L in the range $2{\cdot}17 \cdot 10^{-5}$M to $8{\cdot}00 \cdot 10^{-4}$M at pH 4·25, treated by graphical analysis using equation (*6*) and (*7*) confirmed the validity of equilibrium (*C*). The constant is given in Table II.

The Variation Method in Equimolar Solutions

A component ratio of 1 : 1 was found from the positions of the maxima of the symmetrical variation curves and in evaluation of the data using JOB and KONVAR programs for solutions at pH 4·90, 5·30 and 11·85, $c_0 = 9{\cdot}34 \cdot 10^{-5}$M and λ 490, 516, 525 and 540 nm. The values of the constant are given in Tables II and IV.

Spectrophotometric Titrations

Titration of a $2{\cdot}34 \cdot 10^{-5}$M solution of Pb^{2+} with a PAR solution at pH 10·32 and using λ 490, 515, 525 and 540 nm indicates the formation of a 1 : 1 complex; the molar absorption coefficient is given in Table V.

TABLE V
Molar Absorption Coefficients for the PbL Chelate

Conditions	$\varepsilon \cdot 10^{-4}$, mmol^{-1} cm^2		
	515 nm	525 nm	540 nm
$A = f$(pH) $c_M = 1{\cdot}90 \cdot 10^{-5}$M $p_L = 16{\cdot}1$	4·52[a] 3·83[d]	4·19[a] 3·90[d]	3·63[a] 3·57[b]; 3·76[c] 3·60[d]
$A = f$(pH), pH 6 $c_L = 2{\cdot}44 \cdot 10^{-5}$M $p_M = 10{\cdot}1$	3·55[a]	3·54[a]	3·25[a]
$A = f$(pH) $c_L = c_M = 2{\cdot}44 \cdot 10^{-5}$M	3·77[d]	3·80[d]	3·42[d]
$A = f(c_L)$, pH = 9·53	3·56[d,e]	3·48[d]	3·23[d]
Photometric titration $c_M = 2{\cdot}34 \cdot 10^{-5}$M pH 10·32	3·74[d]	3·68[d]	3·28[d]
Average:	*3·72*[f]	*3·73*[f]	*3·30*[f]

[a] KANKARE program; [b] graphical analysis; [c] PRCEK T200; [d] from the horizontal branch (A/c_M); [e] at 520 nm; [f] from the average value for $p_L = 16{\cdot}1$.

Distribution Diagrams in the Pb^{2+}–PAR *System*

Distribution diagrams of the components were computed using the HALTAFALL program from the equilibrium constant values for the equilibria

$$\begin{aligned}
-\,H^+ + Pb^{2+} + LH_2 &= PbLH^+ & \log k_{11H} &= -\,0{\cdot}12\\
-2\,H^+ + Pb^{2+} + LH_2 &= PbL & \log k_{12} &= -\,6{\cdot}51\\
H^+ + LH_2 &= LH_3^+ & \log K_{a1} &= -\,3{\cdot}03\\
-\,H^+ + LH_2 &= LH^- & \log K_{a2} &= -\,5{\cdot}57\\
-2\,H^+ + LH_2 &= L^{2-} & \log K_{a3} &= -11{\cdot}95
\end{aligned}$$

under conditions: $c_L = 1{\cdot}98 \,.\, 10^{-5}$M, $p_M = 100$ (Fig. 5), $c_M = c_L = 2{\cdot}44 \,.\, 10^{-5}$M (Fig. 6) and $c_M = 1{\cdot}90 \,.\, 10^{-5}$M, $p_L = 16{\cdot}1$ (Fig. 7).

The distribution curves of the Pb^{2+} complexes computed without an assumption of hydrolytic equilibria correspond to the pH curves up to pH 9 for $c_M = c_L$, pH 10 for $p_L = 16{\cdot}1$ and pH 6 for $p_M = 100$. At higher pH values, where the measurement was disturbed by hydrolytic turbidity in solutions with excess Pb^{2+} or by a considerable increase in the absorbance of solutions with excess of the reagent, the validity of the distribution curves of the PbL complex is only theoretical. Analysis of the

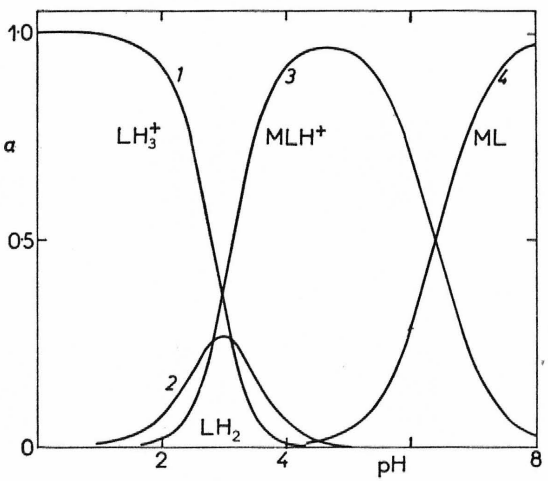

FIG. 5

Distribution Curves of Components in the Pb^{2+}–PAR System for $c_L = 1{\cdot}98 \,.\, 10^{-5}$M and p_M 100

Curve 1 $\alpha = [LH_3^+]/c_L$, 2 $\alpha = [LH_2]/c_L$, 3 $\alpha = [MLH]/c_L$, 4 $\alpha = [ML]/c_L$.

absorbance curves confirmed the presence of complexes $PbLH^+$ and PbL with different state of dissociation of the ligand *p*-hydroxyl group. The earlier assumed

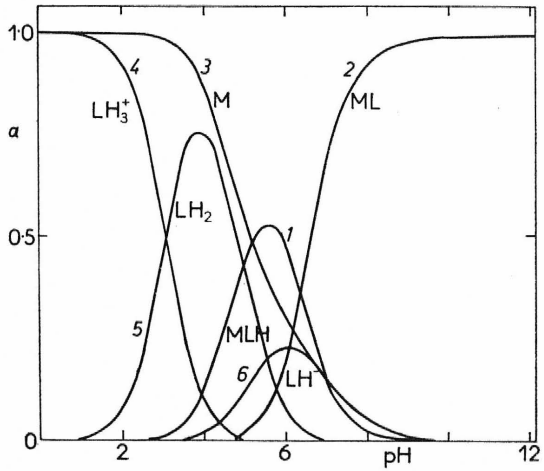

FIG. 6

Distribution Curves of Components in the Pb^{2+}–PAR System PAR for $c_L = c_M = 2{\cdot}44 \cdot 10^{-5}$M

Curve *1* $\alpha = [MLH^+]/c_L$, *2* $\alpha = [ML]/c_L$, *3* $\alpha = [M]/c_L$, *4* $\alpha = [LH_3^+]/c_L$, *5* $\alpha = [LH_2]/c_L$, *6* $\alpha = [LH^-]/c_L$.

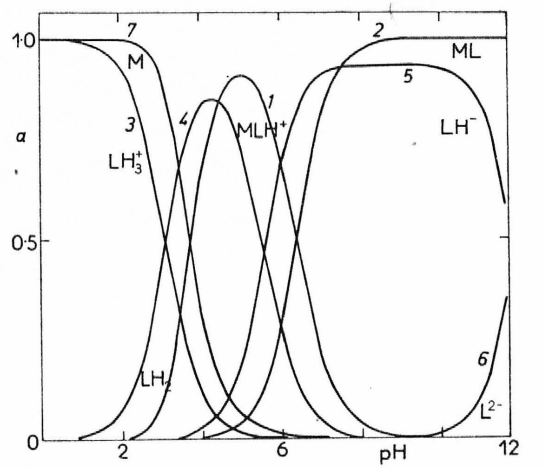

FIG. 7

Distribution Curves of Components in the Pb^{2+}–PAR System for $c_M = 1{\cdot}90 \cdot 10^{-5}$M, p_L 16·1

Curve *1* $\alpha = [MLH^+]/c_M$, *2* $\alpha = [ML]/c_M$, *3* $\alpha = [LH_3^+]/c_L$, *4* $\alpha = [LH_2]/x_L$, *5* $\alpha = [LH^-]/c_L$, *6* $\alpha = [L^{2-}]/c_L$, *7* $\alpha = [M]/c_M$.

TABLE VI

Characteristics of the Pb^{2+} Chelate with 4-(2-Pyridylazo)resorcinol in Aqueous Solutions at 25°C and I 0·1

Chelate	λ_{max} nm	$\varepsilon \cdot 10^{-4}$ $mmol^{-2}$ cm^2	log k	log K	Ref.
$PbLH^+$	515, 410	1·43	−0·12[a]	11·83[b]	this work
	518	3·72[c]	−6·43[d]	10·96[e]	
			−6·52		
$PbLH^+$	512		−0·1[a]	11·9[b,f]	4
1 : 1	520	3·80 . 10			23
1 : 1	520	4·00			3
1 : 1	515			6·5[g]	2
1 : 2[h]	520				4, 6

[a] $k_{11H} = [MLH][H]/[M][LH_2]$; [b] $K_{1H} = [MLH]/[M][LH] = k_{11H}/K_{a3}$; [c] at 515 nm; [d] $k_{12} = [ML][H]^2/[M][LH_2]$; [e] $K_1 = [ML]/[M][L] = k_{12}/K_{a2}K_{a3}$; [f] corrected value; [g] stability constant; [h] the 1 : 2 complex was not found in this work at $c_L \leqq 3{\cdot}0 \cdot 10^{-4}$M and pH ≦ 10.

TABLE VII

Some Characteristics of the Spectrophotometric Calibration Curves for the Determination of Lead with PAR

0·94—5·62 μg Pb^{2+}/ml, $c_L = 4{\cdot}30 \cdot 10^{-4}$M, I 0·1.

pH	λ nm	ε $mmol^{-1}$ cm^2	A_L[a]	s[b] μg/ml	Sensitivity[c] μg/cm^2	U . 10^4[b]
8·80[d]	515	38 260 ± 203	0·309 ± 0·003	0·0263	0·0542	1·18
	520	38 900 ± 188	0·253 ± 0·003	0·0240	0·0533	1·01
	530	37 590 ± 600	0·175 ± 0·010	0·0791	0·0551	10·29
8·38[e]	515	38 120 ± 145	0·304 ± 0·003	0·0200	0·0544	0·68
	520	39 070 ± 163	0·242 ± 0·003	0·0206	0·0530	0·75
	530	38 640 ± 134	0·161 ± 0·003	0·0175	0·0536	0·53

[a] Absorbance blank as the intercept of the regression straight line; [b] estimate of the standard deviation of the scatter of the values around the regression straight line, recalculated to μg/ml. $s = \sqrt{U/(n-2)} \cdot 1000$ at. wt./ε, where $U = \sum(y_{exp} - y_{calc})^2$, number of experimental points $n = 21$, correlation coefficient[24] in the range val 0·99993—0·99997;) [c] sensitivity index according to Sandell[25] for $A = 0{\cdot}010$; [d] 0·05M ammonia buffer; [e] 0·05M borate buffer.

complex with M : L = 1 : 2 (ref.[4]) was not found even in alkaline solutions (pH 10) with excess reagent ($c_L = 3{\cdot}0 \cdot 10^{-3}$M, $c_M = 1{\cdot}90 \cdot 10^{-5}$M). The earlier erroneous deducation on the stoichiometry of the chelate was a result of insufficient experience in interpretation of the absorbance curves and also of use of insufficiently pure reagent.

The characteristics of chelates of Pb^{2+} with PAR including older data are summarized in Table VI.

Spectrophotometric Determination of Pb^{2+} *with* PAR

The spectrophotometric determination of lead is based on the PbL complex with λ_{max} 518 nm and ε_{max} $3{\cdot}7 \cdot 10^4$ in aqueous solutions in the range pH 8·0–8·8. At pH 7·8, the PbLH complex is formed, with lower molar absorption coefficient; at pH > 9 the *o*-hydroxyl group of the reagent dissociates and the absorbance increases (Fig. 4, curve *1*). The pH can be adjusted using tetraborate buffer with a final concentration of 0·05M or ammoniacal buffer with a final concentration of 0·1M. The final reagent concentration in the determination, $c_L = 4{\cdot}30 \cdot 10^{-5}$M, was derived from the $A = d(c_L)$ plots with $c_M = 2{\cdot}80 \cdot 10^{-5}$M at pH 7·25, 8·50 and 9·53. The basic characteristics of the calibration curves for determining Pb^{2+} in the range 0·94–5·62 μg Pb^{2+}/ml in the final solution at pH 8·38 (0·05M tetraborate buffer) and at pH 8·80 (0·05M ammonia buffer) in 1 cm cells were evaluated using the STAT program. Wavelengths of 520 and 530 nm are optimal (Table VII). In contrast to older procedures for determining Pb^{2+} with PAR, recommending an optimal pH value of 10·0, an interval of pH 8–8·8 is chosen in this work; in this range the reagent absorbance is independent of the pH value.

The Effect of Foreign Ions

The determination of Pb^{2+} with PAR under the given conditions (3·13 μg Pb/ml) is not interfered by the presence of KNO_3 (1·0M), $NaClO_4$ (0·8M), NaCl (1·6M), Na_2SO_4 (0·14M) and KBr (1·04M), even when the solution is left to stand 16 hours with the mentioned amount of NaCl or Na_2SO_4. No increased absorbance or change in λ_{max} was observed in the presence of polyvinylalcohol (0·2%), antipyrine ($7{\cdot}5 \cdot 10^{-3}$M), pyrocatechol ($2{\cdot}2 \cdot 10^{-3}$M), sulphosalicylic acid ($2{\cdot}0 \cdot 10^{-3}$M), citrate ($7{\cdot}3 \cdot 10^{-4}$M), tartrate (0·01M), KI (0·13M) or KSCN (0·15M). Most metallic ions interfere strongly in alkaline medium and must be separated prior to the determination.

The authors wish to thank Professor L. Sommer for his interest in this work and for valuable discussions and advice.

REFERENCES

1. Pollard F. H., Hanson P., Geary W.: Anal. Chim. Acta *20*, 26 (1959).
2. Kristiansen H., Langmyhr F. J.: Acta Chem. Scand. *13*, 1473 (1959).
3. Dagnall R. M., West T. S., Young P.: Talanta *12*, 583 (1965).
4. Hniličková M., Sommer L.: This Journal *26*, 2189 (1961).
5. Busev A. L., Tipcová V. G.: Zh. Anal. Khim. *16*, 275 (1961).
6. Geary W. J., Nickless G., Pollard F. H.: Anal. Chim. Acta *26*, 575 (1962).
7. Sommer L., Kubáň V., Havel J.: Folia Fac. Sci. Natur. Univ. Brno (Chemia), Vol. 11, Part *1* (1970).
8. Šteflová Z.: *Thesis.* University Brno, Brno 1975.
9. Likussar W., Boltz D. F.: Anal. Chem. *43*, 1265 (1971).
10. Likussar W.: Anal. Chem. *45*, 1926 (1973).
11. Vošta J.: *Thesis.* University Brno, Brno 1974.
12. Havel J., Vošta J.: Unpublished results.
13. Wallace R. H.: J. Phys. Chem. *64*, 899 (1960).
14. Kankare J. J.: Anal. Chem. *42*, 1322 (1972).
15. Šteflová Z., Havel J.: Unpublished results.
16. Ingri N., Kakolowicz W., Sillén L. G., Warnquist B.: Talanta *14*, 1261 (1967).
17. Havel J.: Scr. Fac. Sci. Natur. Univ. Brno, Chemia *4*, 3 : 117 (1973).
18. Pavlíková N.: *Thesis.* University Brno, Brno 1976.
19. Pavlíková N., Havel J., Horák J.: Scr. Fac. Sci. Natur. Univ. Brno, in press.
20. Langová M.: Unpublished results.
21. Geary W. J., Nickless G., Pollard F. H.: Anal. Chim. Acta *27*, 71 (1962).
22. Russeva E., Kubáň V., Sommer L.: This Journal, in press.
23. Iwamoto T.: Bull. Chem. Soc. Jap. *34*, 605 (1961).
24. Gottschalk G.: *Statistik in der Quantitativen Chemischen Analyse*, p. 49. Enke, Stuttgart 1962.
25. Sandell E. B.: *Colorimetric Determination of Traces of Metals.* Interscience, New York—London 1959.
26. Carell B., Olin A.: Acta Chem. Scand. *16*, 2350 (1962).

Translated by M. Štulíková.